

TCR signal strength controls thymic differentiation of discrete proinflammatory $\gamma\delta$ T cell subsets

Miguel Muñoz-Ruiz^{1,2}, Julie C Ribot², Ana R Grosso², Natacha Gonçalves-Sousa², Ana Pamplona², Daniel J Pennington³, José R Regueiro¹, Edgar Fernández-Malavé^{1,4} & Bruno Silva-Santos^{2,4}

The mouse thymus produces discrete $\gamma\delta$ T cell subsets that make either interferon- γ (IFN- γ) or interleukin 17 (IL-17), but the role of the T cell antigen receptor (TCR) in this developmental process remains controversial. Here we show that *Cd3g^{+/-} Cd3d^{+/-}* (CD3 double-haploinsufficient (CD3DH)) mice have reduced TCR expression and signaling strength on $\gamma\delta$ T cells. CD3DH mice had normal numbers and phenotypes of $\alpha\beta$ thymocyte subsets, but impaired differentiation of fetal V γ 6⁺ (but not V γ 4⁺) IL-17-producing $\gamma\delta$ T cells and a marked depletion of IFN- γ -producing CD122⁺ NK1.1⁺ $\gamma\delta$ T cells throughout ontogeny. Adult CD3DH mice showed reduced peripheral IFN- γ ⁺ $\gamma\delta$ T cells and were resistant to experimental cerebral malaria. Thus, TCR signal strength within specific thymic developmental windows is a major determinant of the generation of proinflammatory $\gamma\delta$ T cell subsets and their impact on pathophysiology.

Proinflammatory cytokines orchestrate protective immune responses to pathogens and tumors but are also responsible for tissue-damaging inflammation and autoimmunity. Among various cellular sources, $\gamma\delta$ T cells have emerged as major producers of IFN- γ and/or IL-17 in several diseases. On one hand, IFN- γ production by $\gamma\delta$ T cells underlies protective responses to infections¹, as well as tumor immunity², but it is also associated with susceptibility to severe malaria³. On the other hand, IL-17 secretion by $\gamma\delta$ T cells is a key defense mechanism against various bacterial infections, such as *Staphylococcus aureus*⁴ or *Listeria monocytogenes*^{4,5}, but is also a critical component of inflammatory and autoimmune syndromes such as psoriasis^{6–8}, colitis⁹, chronic granulomatous disease¹⁰, ischemic brain inflammation¹¹ and experimental autoimmune encephalomyelitis^{12–14}.

The nonredundant roles of IFN- γ -producing (IFN- γ ⁺) and IL-17⁺ $\gamma\delta$ T cells are tightly linked to “developmental preprogramming” in the mouse thymus¹⁵. Whereas conventional effector CD4⁺ T cells differentiate in peripheral lymphoid organs in response to antigen and additional environmental cues, $\gamma\delta$ T cells complete their functional maturation in the thymus. The mouse, which generates discrete populations of IFN- γ ⁺ and IL-17⁺ $\gamma\delta$ T cells that can be identified on the basis of CD27 and CCR6 expression^{12,16,17}. Importantly, these subpopulations have different functions; for example, CD27–IL-17⁺ $\gamma\delta$ T cells promote tumor cell growth^{18,19}, whereas CD27⁺IFN- γ ⁺ $\gamma\delta$ T cells inhibit it^{2,20}. It is therefore crucial to understand how distinct functional $\gamma\delta$ T cell subsets are generated and regulated.

Given its pivotal role in thymocyte development and selection, the TCR is a likely determinant of the functional differentiation of $\gamma\delta$ T cells¹⁵. It was shown that $\gamma\delta$ T cells specific for the major

histocompatibility (MHC) complex I molecules T10 and T22 (T10/T22), which account for ~0.4% of peripheral $\gamma\delta$ T cells, produce IL-17 and IFN- γ in the absence and presence, respectively, of thymic T10/T22 expression¹². Consistent with this, thymic selection drives dendritic epidermal T cells (DETCs) that populate the mouse epidermis toward IFN- γ but away from IL-17 production²¹. However, SKG mice, which are hypomorphic for the TCR signal-transducing kinase ZAP70 and retain only 10% of its signaling ability, show impaired development of IL-17⁺ $\gamma\delta$ T cells²². As such, the role of TCR signal ‘strength’ in the development of proinflammatory $\gamma\delta$ T cell subsets remains unclear.

TCR signal strength is known to control the earliest stage of $\gamma\delta$ T cell development, i.e., lineage commitment²³. The manipulation of signal transduction in TCR-transgenic T cells influences the $\gamma\delta$ versus $\alpha\beta$ thymocyte fate^{24,25}, with $\gamma\delta$ T cells requiring stronger TCR signaling than $\alpha\beta$ T cells to develop; however, the impact on subsequent maturation of $\gamma\delta$ T cells, particularly IFN- γ ⁺ versus IL-17⁺ $\gamma\delta$ T cells, was not assessed in these studies. Models based on a single transgenic TCR may not be ideal to answer this question, however, because $\gamma\delta$ T cell development is tightly linked to the dynamics of TCR rearrangements during ontogeny. Indeed, ‘developmental waves’ with distinct TCR gene usage populate different peripheral tissues, and distinct TCR γ chain variable region (V γ) repertoires can have substantial biases toward IFN- γ or IL-17 production^{16,26}. For example, of the two main $\gamma\delta$ T cell subsets in peripheral lymphoid organs, V γ 1⁺ T cells preferentially secrete IFN- γ , whereas V γ 4⁺ T cells are biased toward IL-17 (refs. 16,26). In addition, V γ 5⁺ T cells generated around embryonic days 15–16 (E15–E16) do not secrete IL-17, whereas this

¹Department of Immunology, School of Medicine, Complutense University, Madrid, Spain. ²Instituto de Medicina Molecular, Faculdade de Medicina, Universidade de Lisboa, Lisbon, Portugal. ³Blizard Institute, Barts and The London School of Medicine, Queen Mary University of London, London, UK. ⁴These authors contributed equally to this work. Correspondence should be addressed to B.S.-S. (bssantos@medicina.ulisboa.pt) or E.F.-M. (edfern@med.ucm.es).

Received 7 December 2015; accepted 1 March 2016; published online 4 April 2016; doi:10.1038/ni.3424

cytokine is abundantly produced by $V\gamma 6^+$ T cells that differentiate at E17–E18. Moreover, in-depth transcriptional profiling of $\gamma\delta$ thymocyte subsets by the Immunological Genome Project (<http://www.immgen.org>) demonstrates a divergence between the transcriptional networks of IL-17-biased $V\gamma 6^+$ and $V\gamma 4^+$ T cells versus IFN- γ -biased $V\gamma 5^+$ and $V\gamma 1^+$ T cells^{27,28}.

The association between certain $\gamma\delta$ TCR repertoires and differential IFN- γ or IL-17 production²⁶ suggests that TCR signaling is a major determinant of the functional differentiation of $\gamma\delta$ T cells in the thymus. However, testing this hypothesis has been hampered by the lack of mouse models that specifically interfere with TCR $\gamma\delta$ signaling *in vivo*. Here we describe a selective defect in the surface expression of TCR $\gamma\delta$, but not TCR $\alpha\beta$, in $Cd3g^{+/-} Cd3d^{+/-}$ (CD3DH) mice and show that reduced TCR $\gamma\delta$ signaling affects the differentiation of discrete subsets of IFN- γ and IL-17 $\gamma\delta$ T cells during thymic ontogeny, with pathological consequences.

RESULTS

CD3DH mice show reduced TCR signaling in $\gamma\delta$ T cells

During the screening of various lines of (single or double) haploinsufficient CD3 mutants, we observed that CD3DH mice had markedly lower cell surface expression of TCR $\gamma\delta$ and CD3 ϵ (Fig. 1a,b) than did wild-type mice, as well as low $\gamma\delta$ thymocyte numbers (Fig. 1c). This reduction was not observed in singly haploinsufficient ($Cd3d^{+/-}$ or $Cd3g^{+/-}$) mice (Supplementary Fig. 1a) and was more severe than that observed in CD3 δ -deficient ($Cd3d^{-/-}$) mice²⁹ (Supplementary Fig. 1b). The reduced numbers of $\gamma\delta$ thymocytes in CD3DH mice were not due to increased cell death (Supplementary Fig. 1c), which suggests that lower TCR $\gamma\delta$ expression impaired $\gamma\delta$ T cell development, as reported in transgenic models^{24,25}. CD3DH $\gamma\delta$ thymocytes remained mostly CD4⁻CD8⁻ (data not shown), thus excluding diversion into the $\alpha\beta$ lineage. However, TCR $\alpha\beta$ expression was not affected, and $\alpha\beta$ thymocyte development proceeded normally in CD3DH mice (Fig. 1d–f). Consistent with normal TCR $\alpha\beta$ signaling and selection, the generation of agonist-selected Fopx3⁺CD4⁺ and CD1d-restricted natural killer T (NKT) cells was similar to that in wild-type mice (Supplementary Fig. 1d,e).

To characterize the downstream effects of reduced TCR $\gamma\delta$ expression, we assessed the expression of the agonist selection markers CD73, a signature of TCR $\gamma\delta$ signaling during thymic development³⁰, and CD5, a stable indicator of TCR signal strength³¹, as well as the maturation markers CD122 and CD44 (refs. 12,15,17). All were markedly lower in $\gamma\delta$ thymocytes from CD3DH mice compared to those from wild-type mice (Fig. 1g). Upon TCR stimulation, the activation markers CD69 and CD25 were also decreased in peripheral (splenic) CD3DH $\gamma\delta$ T cells (Fig. 1h). Moreover, CD3DH $\gamma\delta$ T cells had lower TCR responsiveness, as assessed by activation of the kinases ERK (Fig. 1i) and AKT (Supplementary Fig. 2a) and calcium mobilization (Supplementary Fig. 2b), than wild-type $\gamma\delta$ T cells. These data indicate that lower surface TCR $\gamma\delta$ expression in CD3DH mice impairs signal transduction and downstream TCR-dependent processes.

To test whether the phenotype of $\gamma\delta$ T cells in CD3DH mice was cell intrinsic, we established mixed (1:1) bone marrow (BM) chimeras by transferring CD3DH (Thy-1.2) and wild-type (Thy-1.1) whole BM cells into either TCR δ -deficient or RAG2-deficient hosts. In both hosts we observed reduced TCR $\gamma\delta$ expression in CD3DH-derived $\gamma\delta$ thymocytes (Fig. 1j), which consistently accounted for a minor fraction of the total $\gamma\delta$ thymocyte pool, compared to wild-type $\gamma\delta$ thymocytes. In contrast, $\alpha\beta$ thymocytes were generated in similar numbers from CD3DH and wild-type precursors (Fig. 1k), indicating that CD3DH progenitors are outcompeted by wild-type precursors

for $\gamma\delta$ but not $\alpha\beta$ T cell development. Of note, this defect could be overcome with a 1:9 (wild-type/CD3DH) ratio (Supplementary Fig. 3), which indicates that CD3DH progenitors can generate $\gamma\delta$ thymocytes, albeit with lower potency than wild-type precursors. Thus, haploinsufficiency for both $Cd3d$ and $Cd3g$ results in lower TCR $\gamma\delta$ expression levels and signaling and reduced numbers of $\gamma\delta$ thymocytes.

Impaired differentiation of IL-17⁺ and IFN- γ ⁺ $\gamma\delta$ T cells

We next analyzed the functional differentiation of $\gamma\delta$ T cell subsets. Development of CD27⁺ and CD27⁻ $\gamma\delta$ T cells was observed during the embryonic stages and continued into adulthood (Fig. 2a), as previously reported¹⁶. Both IFN- γ ⁺ and IL-17⁺ $\gamma\delta$ thymocytes were observed in lower frequencies in CD3DH than in wild-type E18 embryos (Fig. 2b,c). Whereas the reduction in IFN- γ ⁺ $\gamma\delta$ thymocytes was maintained after birth and into adulthood, the frequency of IL-17⁺ $\gamma\delta$ thymocytes in CD3DH mice normalized to wild-type levels between 1 and 6 weeks of age (Fig. 2b–d). This coincided with a switch in TCR V γ usage: most IL-17⁺ $\gamma\delta$ T cells were V $\gamma 1$ ⁻V $\gamma 4$ ⁻ (validated as V $\gamma 6$ ⁺ by GL3 and 17D1 antibody staining)¹⁸ (data not shown) in E18 embryos and neonates and V $\gamma 4$ ⁺ from week 1 on (Fig. 2e). Of note, IL-17⁺V $\gamma 6$ ⁺ cells are generated exclusively during embryonic life³²; we found that only V $\gamma 6$ ⁺ (not V $\gamma 4$ ⁺) thymocytes showed reduced IL-17 production in CD3DH mice (Fig. 2f). These data suggest that the effector $\gamma\delta$ T cell subsets generated within distinct developmental windows, as marked by particular V γ usage, have distinct TCR signal strength requirements.

Transcriptional signatures of TCR signal strength in $\gamma\delta$ T cells

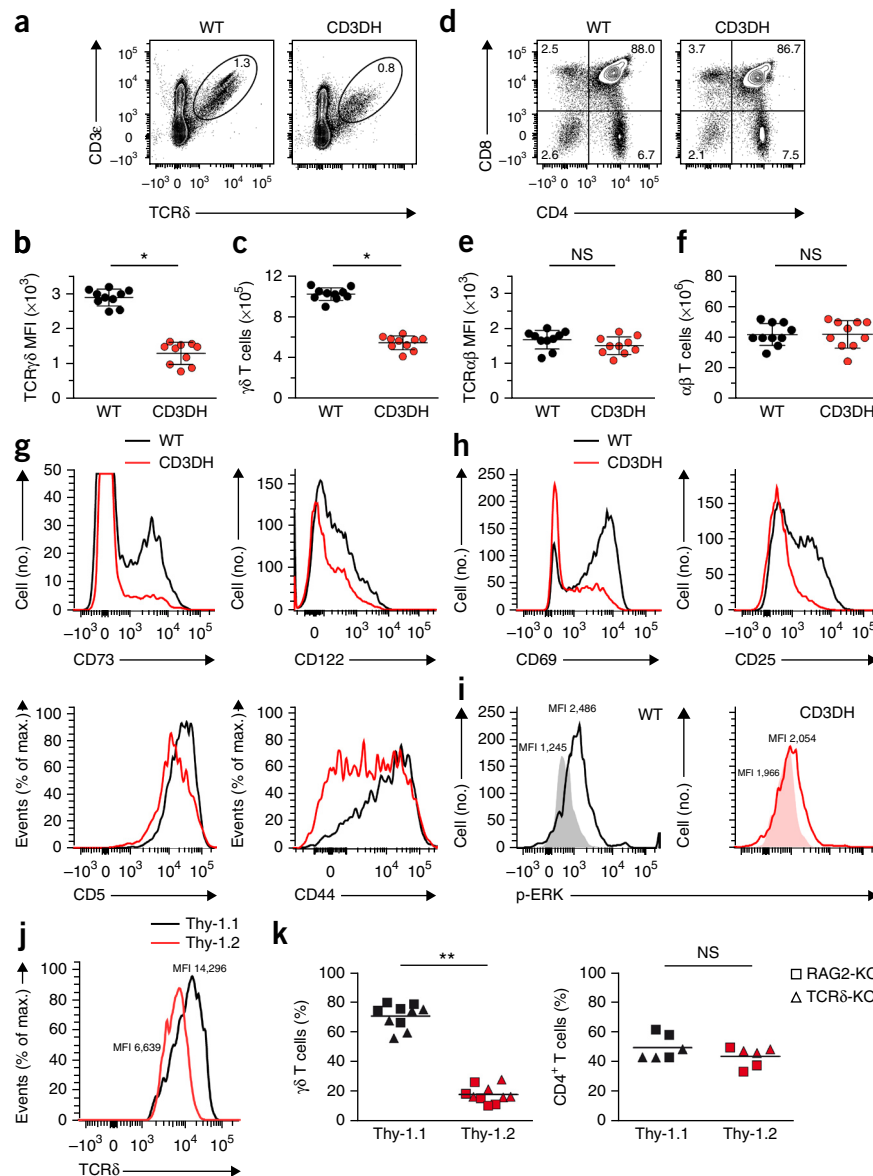
Because developmental programming of $\gamma\delta$ T cells is set at the transcriptional level^{27,33,34}, we performed transcriptome-wide analysis of sorted total $\gamma\delta$ thymocytes from CD3DH and wild-type E18 and 6-week-old mice. This analysis showed highly dynamic patterns of gene expression during ontogeny (Fig. 3a). Among the mRNAs upregulated in $\gamma\delta$ thymocytes from E18 to adult in wild-type mice, those linked to IFN- γ production were generally impaired in CD3DH $\gamma\delta$ thymocytes and included *Nr4a3*, *Nr4a2* and *Bcl2a1* (refs. 16,34,35); the transcription factors *Egr2*, *Egr3* and *Id3*, which are major suppressors of the IL-17 differentiation pathway²¹; and *Nfkbiz* (which encodes the transcription factor I κ B ζ)³⁶, *Tnfrsf18* (encoding GITR), *Lilr4b* (also known as *Gp49a*) and *Lilr4a* (also known as *Lilrb4*, encoding Gp49b)³⁷ (Fig. 3a and Supplementary Fig. 4a).

Key genes involved in IL-17 production, such as *Il17a*, *Il17f* and *Il23r*^{13,33}, which are highly expressed in fetal $\gamma\delta$ thymocytes and reduced in adult $\gamma\delta$ thymocytes in wild-type mice, were downregulated in CD3DH $\gamma\delta$ thymocytes (Fig. 3a). In both wild-type and CD3DH $\gamma\delta$ thymocytes, embryonically rearranged TCRs such as V $\gamma 5$ and V $\gamma 6$ were downregulated, as was the transcription factor PLZF (encoded by *Zbtb16*), which is characteristic of fetal $\gamma\delta$ thymocytes²⁷ (Fig. 3a).

The IL-17⁺ $\gamma\delta$ T cell signature genes *Sox4* and *Sox13* (refs. 27,28) were greatly reduced in embryonic V $\gamma 6$ ⁺ but not V $\gamma 4$ ⁺ CD3DH thymocytes (as compared to wild-type thymocytes) (Supplementary Fig. 4b), indicating that the IL-17⁺V $\gamma 6$ ⁺ and IL-17⁺V $\gamma 4$ ⁺ thymocyte subsets have distinct developmental TCR signal strength requirements. Of note, the expression of *Tbx21* (which encodes T-bet) and *Rorc* (which encodes ROR γ t), which transcriptionally regulate *Ifng* and *Il17a* expression, respectively, was not affected in CD3DH $\gamma\delta$ thymocytes (data not shown).

Next, for a TCR-mediated gain-of-function approach, we stimulated total $\gamma\delta$ thymocytes from adult CD3DH or wild-type mice with

Figure 1 $\gamma\delta$ T cells from CD3DH mice show reduced TCR $\gamma\delta$ expression and signaling. (a) Flow cytometry analysis of CD3 ϵ and TCR δ expression in thymocytes from 1-week-old wild-type (WT) or CD3DH mice ($n = 10$ mice per group). (b–f) TCR $\gamma\delta$ mean fluorescence intensity (MFI) (b) and $\gamma\delta$ thymocyte numbers (c), gated as in a; CD8 versus CD4 phenotypes of thymocytes ($n = 3$ adult mice per group of adult mice) (d), TCR $\alpha\beta$ MFI (e) and absolute numbers of TCR β^+ CD3 $^+$ thymocytes (f) from WT and CD3DH mice. (g) Expression of various agonist selection and maturation markers in gated TCR δ^+ CD3 $^+$ CD27 $^+$ thymocytes. (h) CD69 and CD25 expression in sorted TCR δ^+ CD3 $^+$ CD27 $^+$ spleen cells stimulated with plate-coated anti-CD3 ϵ for 24 h. (i) Analysis of phosphorylated Erk1 and Erk2 (p-ERK; open histograms) versus isotype-matched background staining (shaded histograms) in sorted TCR δ^+ CD3 $^+$ CD27 $^+$ lymph node cells stimulated for 5 min with soluble anti-CD3 ϵ . Data in i are representative of three independent experiments. (j, k) Flow cytometry analysis of comparative TCR $\gamma\delta$ MFI (j) and Thy-1.1 (WT-derived) versus Thy-1.2 (CD3DH-derived) fractions among gated TCR δ^+ CD3 $^+$ and CD4 $^+$ CD3 $^+$ thymocytes (k) from 1:1 mixed WT:CD3DH bone marrow chimeras. Each symbol represents one RAG2-knockout (RAG2-KO) or TCR δ -KO host. Numbers in outlined areas or quadrants of flow cytometry plots indicate percentages of cells in each. In b, c, e and f, points represent individual mice ($n = 10$), and error bars represent mean \pm s.d. NS, not significant; * $P < 0.01$ (Student's *t*-test).



satürating amounts of monoclonal anti-CD3 ϵ for 16 h to achieve crosslinking of all available TCR complexes on the cell surface. We observed an upregulation of *Egr2* and *Egr3* expression in wild-type $\gamma\delta$ thymocytes (Fig. 3b), consistent with their induction by strong TCR signals²¹. *Egr2* and *Egr3* upregulation was also observed in stimulated CD3DH $\gamma\delta$ thymocytes (Fig. 3b), which suggests that increasing $\gamma\delta$ TCR signaling can rescue the expression of IFN- γ -associated transcriptional signatures in CD3DH $\gamma\delta$ thymocytes. In addition, anti-CD3 ϵ stimulation downregulated IL-17 $^+$ $\gamma\delta$ T cell signature genes, such as *Sox4* (ref. 28), *Il23r* and *Il1r1* (refs. 13,33,38), in both wild-type and CD3DH $\gamma\delta$ thymocytes (Fig. 3b). Collectively, these data suggest that strong TCR signals are required to promote IFN- γ at the expense of IL-17 production by adult $\gamma\delta$ thymocytes.

CD3DH mice lack IFN- γ^{hi} CD122 $^+$ NK1.1 $^+$ $\gamma\delta$ thymocytes

We next tested whether the deficiency in IFN- γ expression in $\gamma\delta$ thymocytes from CD3DH mice involved the depletion of a specific $\gamma\delta$ T cell subset committed to IFN- γ production. Thus, we analyzed the expression of CD122 (ref. 12) and NK1.1 (refs. 17,30), two markers previously associated with IFN- γ^+ $\gamma\delta$ T cells, on adult CD27 $^+$ $\gamma\delta$ T cells. We detected a CD122 $^+$ NK1.1 $^+$ $\gamma\delta$ T cell population in the wild-type thymus that was absent in CD3DH mice (Fig. 4a,b). CD122 $^+$ NK1.1 $^-$ $\gamma\delta$ T cells, probably precursors of CD122 $^+$ NK1.1 $^+$ $\gamma\delta$ T cells, were also reduced in the CD3DH thymus compared to the wild-type thymus (Fig. 4a). The V γ repertoire changed from V γ 4-biased to V γ 1-enriched between the CD122 $^-$ and the more mature CD122 $^+$ $\gamma\delta$

T cells in wild-type thymi (Fig. 4c), which suggests that TCR selection shapes the mature $\gamma\delta$ thymocyte pool. Furthermore, consistent with a requirement for strong TCR signaling, wild-type CD122 $^+$ NK1.1 $^+$ $\gamma\delta$ thymocytes had high expression of the selection markers CD44, CD73 and CD45RB, which were not detected on CD122 $^-$ $\gamma\delta$ thymocytes (Fig. 4d). Notably, wild-type CD122 $^+$ NK1.1 $^+$ $\gamma\delta$ thymocytes had the highest expression of IFN- γ (Fig. 4d), suggesting that the IFN- γ^{hi} $\gamma\delta$ T cells have a differentiation defect in CD3DH mice. Furthermore, in mixed (wild-type and CD3DH) BM chimeras, CD27 $^+$ CD122 $^+$ NK1.1 $^+$ $\gamma\delta$ thymocytes were generated exclusively from wild-type progenitors (Fig. 4e). We observed this in both 1:1 and 1:9 (wild-type/CD3DH) chimeras (Fig. 4e), indicating a strong competitive disadvantage of CD3DH precursors along this developmental pathway.

We next aimed to rescue the generation of CD122 $^+$ NK1.1 $^+$ $\gamma\delta$ thymocytes in CD3DH mice by crosslinking the TCR complex *in vivo*. Intraperitoneal injection of the antibody 17A2, which crosslinks CD3 ϵ γ dimers, rescued CD122 $^+$ NK1.1 $^+$ $\gamma\delta$ thymocyte development in CD3DH mice, leading to frequencies similar to that in wild-type mice (Fig. 4f,g). Moreover, wild-type mice treated with 17A2 showed an increase in CD122 $^+$ NK1.1 $^+$ $\gamma\delta$ thymocytes, as compared to untreated

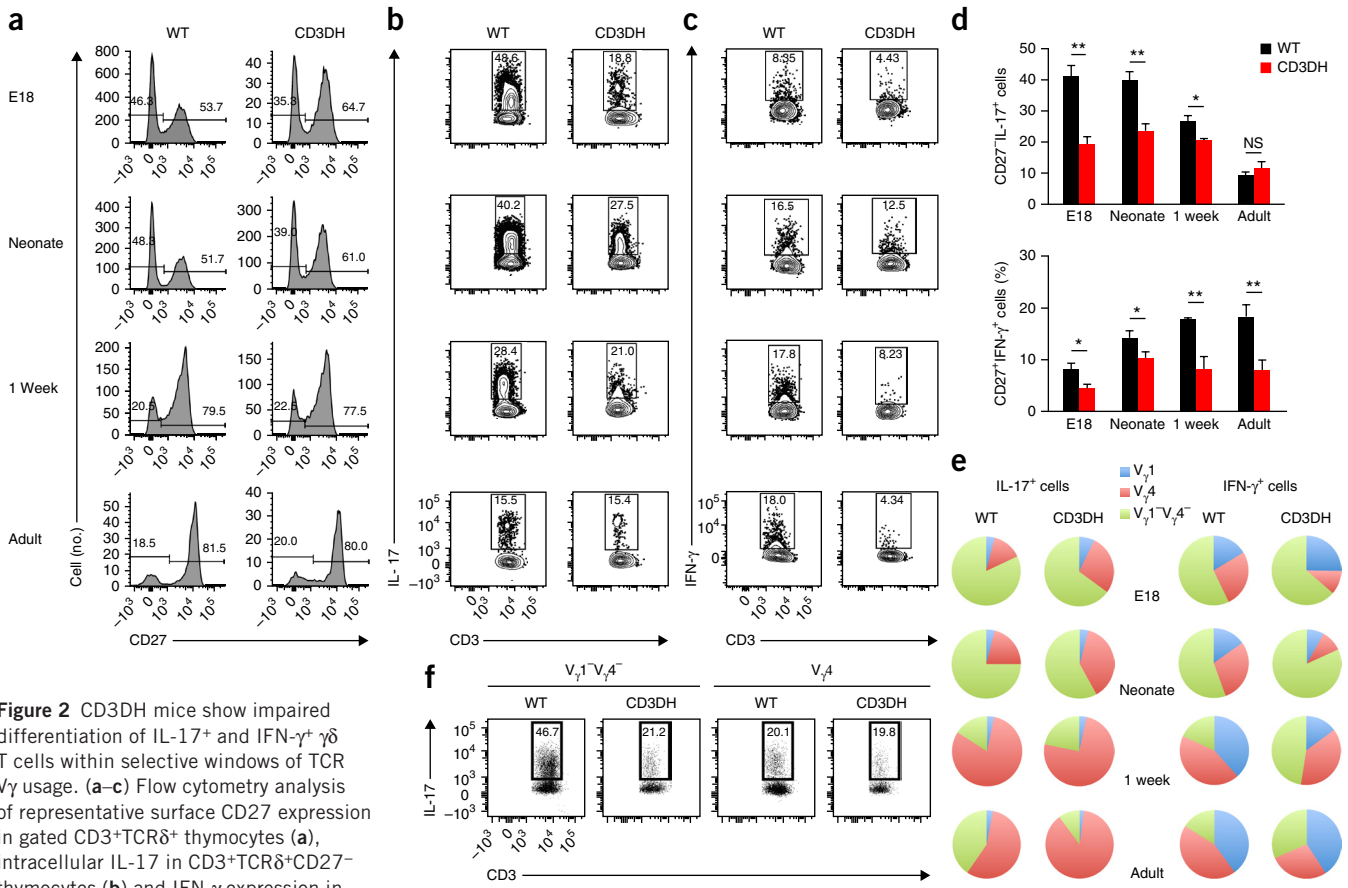


Figure 2 CD3DH mice show impaired differentiation of IL-17⁺ and IFN- γ ⁺ $\gamma\delta$ T cells within selective windows of TCR V γ usage. **(a–c)** Flow cytometry analysis of representative surface CD27 expression in gated CD3⁺TCR δ ⁺ thymocytes **(a)**, intracellular IL-17 in CD3⁺TCR δ ⁺CD27⁻ thymocytes **(b)** and IFN- γ expression in CD3⁺TCR δ ⁺CD27⁺ thymocytes **(c)** from wild-type (WT) or CD3DH mice at various developmental stages after stimulation with PMA and ionomycin. Numbers indicate the percentages cells in the bracketed region. **(d)** Percentage of CD27⁺IL-17⁺ (top) and CD27⁺IFN- γ ⁺ (bottom) $\gamma\delta$ T cells in WT and CD3DH mice determined as in **b** and **c**, respectively. NS, not significant; * P < 0.05; ** P < 0.01 (Student's t -test). Data are mean \pm s.d.; n = 16 E18 embryos, 6 neonates, 5 1-week-old and 10 adult mice. **(e)** V γ usage by CD27⁺IL-17⁺ or CD27⁺IFN- γ ⁺ $\gamma\delta$ T cells at various developmental stages (n = 7 mice per group), as determined by flow cytometry. **(f)** Flow cytometry analysis of intracellular IL-17 expression in CD3⁺TCR δ ⁺CD27⁻ thymocytes sorted from three pooled E18 WT or CD3DH mice after stimulation with PMA and ionomycin. Numbers in outlined areas or quadrants of flow cytometry plots indicate percentages of cells in each. Data are representative of 2–4 experiments per developmental stage.

wild-type mice (**Fig. 4a,f**). These data indicate that strong TCR signaling promotes (and is required for) the development of the IFN- γ ^{hi}CD27⁺CD122⁺NK1.1⁺ $\gamma\delta$ thymocyte subset.

Reduced IFN- γ ⁺ $\gamma\delta$ T cells and cerebral malaria resistance

We next investigated the consequences of reduced $\gamma\delta$ TCR signaling in CD3DH mice on peripheral $\gamma\delta$ T cells. Upon *ex vivo* stimulation with phorbol ester (PMA) and ionomycin, CD3DH splenocytes showed reduced CD27⁺IFN- γ ⁺ but normal CD27⁻IL-17⁺ $\gamma\delta$ T cell frequencies compared to wild-type splenocytes (**Fig. 5a,b**). In contrast, CD3DH CD4⁺ $\alpha\beta$ T cells differentiated normally into type 1 helper T (T_H1) cells when activated in the presence of IL-12 (**Supplementary Fig. 5**), indicating that the IFN- γ defect of CD3DH mice was selective for $\gamma\delta$ T cells. Moreover, CD27⁺CD122⁺NK1.1⁺CD44⁺ $\gamma\delta$ splenocytes were absent in CD3DH mice but not wild-type mice (**Fig. 5c–f**). We also observed this in competitive wild-type and CD3DH BM chimeras at 1:1 and 1:9 (wild-type/CD3DH) ratios (**Fig. 5e**).

We next assessed the physiological importance of IFN- γ ⁺ CD27⁺CD122⁺ NK1.1⁺ $\gamma\delta$ T cells in a model of cerebral malaria, which is associated with IFN- γ -dependent pathology and a major contribution from $\gamma\delta$ T cells^{3,39}. We induced experimental cerebral malaria with *Plasmodium berghei* ANKA sporozoites, establishing

liver-stage infection, which precedes the symptomatic blood-stage infection. We observed an abundant IFN- γ ⁺ $\gamma\delta$ T cell population in the spleen at day 5 after infection (blood stage) in wild-type mice that was markedly reduced in CD3DH mice (**Fig. 5g**), which also showed higher parasitemia (measured as percentage of infected red blood cells) than infected wild-type mice (**Fig. 5h**). Neurological symptoms appeared in wild-type mice around day 6 after infection and became fatal in all animals by day 7–10 (**Fig. 5i**). By contrast, $\gamma\delta$ T-cell-deficient (TCR δ -deficient) and most CD3DH mice remained healthy and survived (**Fig. 5i**). These data demonstrate that IFN- γ ⁺ $\gamma\delta$ T cells make mice highly susceptible to fatal inflammatory syndromes such as severe malaria.

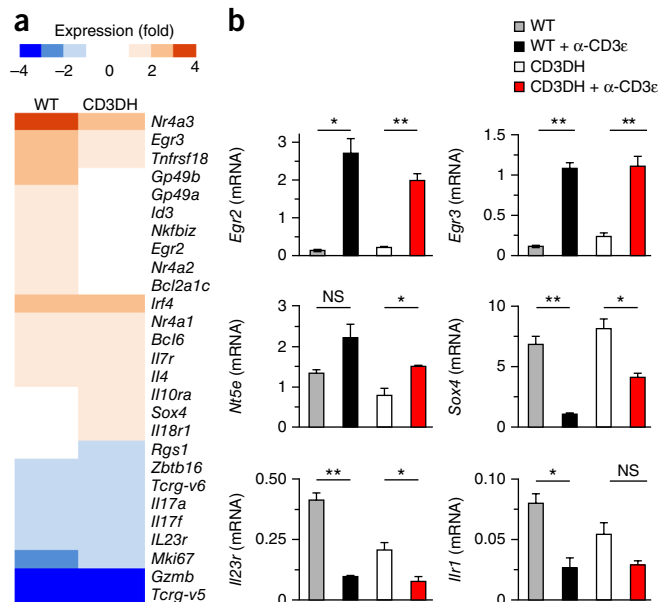
DISCUSSION

The reduced TCR $\gamma\delta$ expression on the surface of $\gamma\delta$ thymocytes in CD3DH mice allowed us to examine a diverse, polyclonal TCR $\gamma\delta$ repertoire, which is highly valuable given the association between specific TCR gene usage and functional differentiation biases²⁶. Our results suggest that distinct developmental $\gamma\delta$ T cell subsets defined by V γ rearrangement and usage have distinct TCR signal strength requirements for differentiation into IFN- γ ⁺ or IL-17⁺ cells.

Figure 3 Transcriptional signatures of TCR signal strength in $\gamma\delta$ thymocytes. (a) Microarray heatmap of differentially expressed genes during ontogeny in sorted CD3⁺TCR δ ⁺ $\gamma\delta$ thymocytes from wild-type (WT) and CD3DH mice (>2-fold enriched in adult relative to fetal thymocytes). (b) Real-time reverse transcription PCR analysis of fold expression (normalized to the housekeeping gene *Hprt*) of *Egr2*, *Egr3*, *Nt5e* (encoding CD73), *Sox4*, *Il23r* and *Ilr1* in sorted CD3⁺TCR δ ⁺ $\gamma\delta$ thymocytes from WT and CD3DH mice ($n = 3$ per group) before and after 16 h stimulation with α -CD3 ϵ (10 μ g/ml). * $P < 0.05$; ** $P < 0.01$ (Student's *t*-test). Data are mean \pm s.d. Data are representative of two independent experiments.

CD3 δ has been shown to be absent from mouse mature TCR $\gamma\delta$ complexes^{40,41}, which raises the question how it affects surface TCR $\gamma\delta$ expression. As we found no evidence for the presence of CD3 δ on the surface of $\gamma\delta$ thymocytes (data not shown), it is unclear whether CD3 δ transiently participates in intracellular TCR $\gamma\delta$ assembly. It is also possible that changes in the relative intracellular amounts of CD3 chains, as observed in CD3DH mice, could cause abnormal glycosylation of CD3 δ ^{42,43} (data not shown) and/or CD3 γ ⁴⁴, which in turn could impair the assembly and stability of nascent TCR complexes, and ultimately their surface expression and signaling^{44,45}.

TCR signaling strength affects thymic commitment to the $\alpha\beta$ versus $\gamma\delta$ lineages^{23–25}. Consistent with this, CD3DH mice showed reduced numbers of total $\gamma\delta$ thymocytes, including loss of IFN- γ ^{hi} CD122⁺NK1.1⁺ $\gamma\delta$ T cells. The number and frequencies of $\alpha\beta$ T cell subsets, including thymic regulatory (T_{reg}) and invariant NKT (iNKT) cells, was normal in CD3DH mice, although the repertoire of TCR $\alpha\beta$ ⁺ subpopulations was not assessed. However, the expression of the $\alpha\beta$



TCR was normal in developing CD3DH thymocytes, indicating that the reduction in TCR expression was specific to $\gamma\delta$ thymocytes.

Notably, whereas IL-17⁺V γ 6⁺ cells were underrepresented in CD3DH mice, their IL-17⁺V γ 4⁺ counterparts were not affected, consistent with distinct developmental requirements for the two IL-17⁺ $\gamma\delta$ T cell

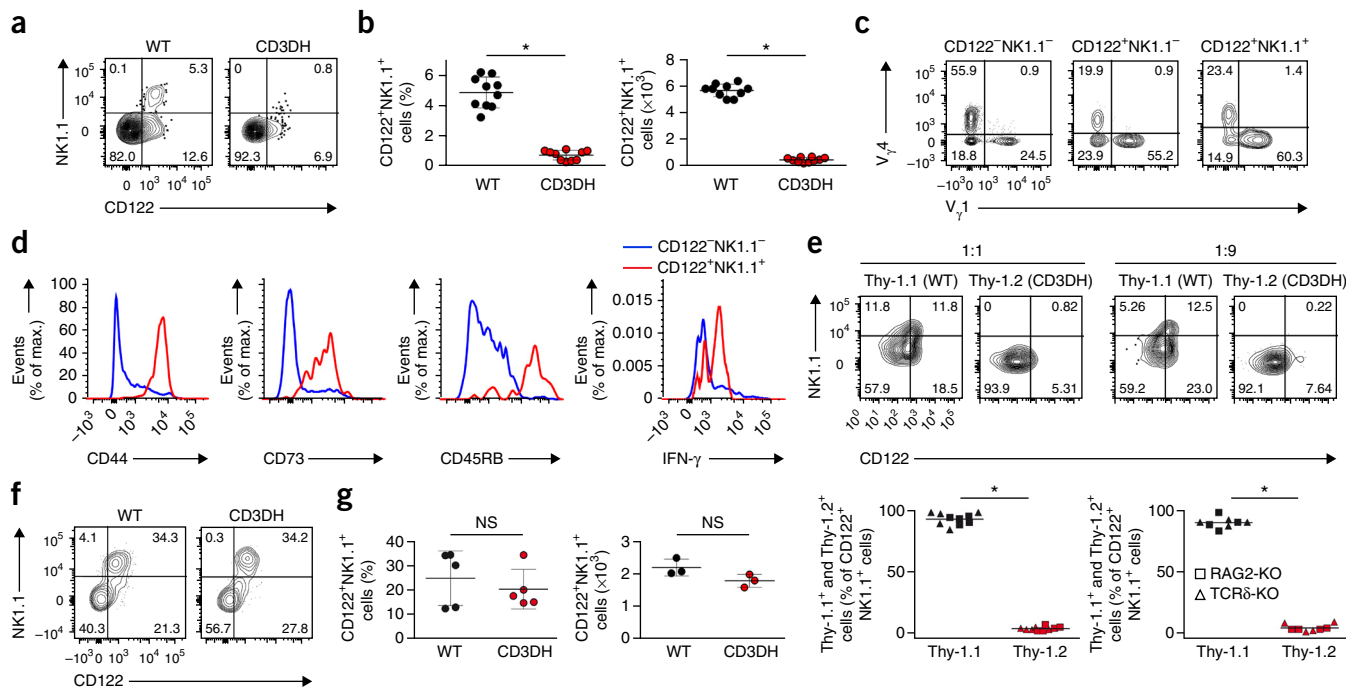


Figure 4 CD3DH mice lack IFN- γ ^{hi}CD122⁺NK1.1⁺ thymocytes, which are rescued by CD3 crosslinking *in vivo*. (a) Flow cytometry analysis of NK1.1 versus CD122 expression in TCR δ ⁺CD3⁺CD27⁺ thymocytes isolated from adult wild-type (WT) or CD3DH mice ($n = 10$ mice per group). (b) Frequencies (left) and total numbers (right) of TCR δ ⁺CD3⁺CD27⁺CD122⁺NK1.1⁺ thymocytes. Each dot represents an individual mouse (10 per group). (c,d) Flow cytometry analysis of V γ 1 versus V γ 4 chain usage (c) and surface CD44, CD73, CD45RB or intracellular IFN- γ production (d) by TCR δ ⁺CD3⁺CD27⁺ thymocyte subsets from adult WT mice ($n = 5$ per group). Data in a–d are representative of at least three independent experiments. (e) Flow cytometry analysis of NK1.1 versus CD122 expression (top) in Thy-1.1⁺ (WT-derived) or Thy-1.2⁺ (CD3DH-derived) fractions (bottom) of TCR δ ⁺CD3⁺CD27⁺CD122⁺NK1.1⁺ thymocytes from 1:1 or 1:9 mixed BM chimeras. Each symbol indicates one RAG2-deficient (RAG2-KO) or TCR δ -KO mouse. (f,g) Flow cytometry showing representative NK1.1 versus CD122 expression (f) and percentage (g, left) and numbers (g, right) of TCR δ ⁺CD3⁺CD27⁺CD122⁺NK1.1⁺ thymocytes in WT or CD3DH mice, 5 d after intraperitoneal injection of α -CD3 17A2 ($n = 3$ per group). Each dot in g represents an individual mouse. NS, not significant; * $P < 0.01$ (Student's *t*-test); error bars indicate mean \pm s.d. Numbers in outlined areas or quadrants of flow cytometry plots indicate percentages of cells in each.

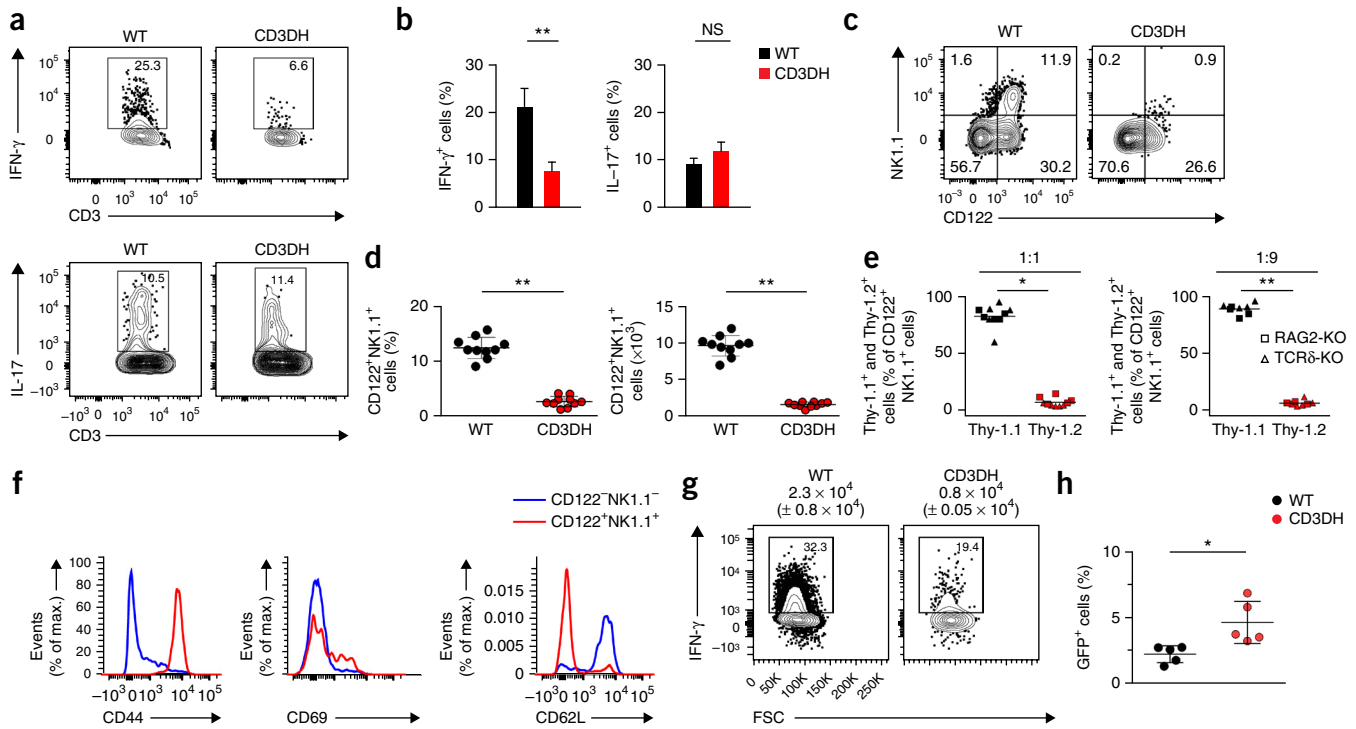


Figure 5 CD3DH mice show reduced peripheral IFN- γ ⁺ $\gamma\delta$ T cells and are resistant to cerebral malaria. (a,b) Flow cytometry analysis (a) and quantification (b) of intracellular IFN- γ and IL-17 expression in CD27⁺ (a, top) and CD27⁻TCR δ ⁺CD3⁺ (a, bottom) splenocytes from adult mice stimulated with PMA and ionomycin. $n = 5$ wild-type (WT) and 8 CD3DH mice per group (b). (c,d) Flow cytometry analysis (c) and quantification (d) of NK1.1 versus CD122 expression in TCR δ ⁺CD3⁺CD27⁺ adult mouse splenocytes. $n = 10$ mice per group (d). (e) Thy-1.1 (WT-derived) versus Thy-1.2 (CD3DH-derived) fractions among TCR δ ⁺CD3⁺CD27⁺CD122⁺NK1.1⁺ splenocytes from 1:1 or 1:9 (WT/CD3DH) mixed BM chimeras. Each symbol indicates one RAG2-deficient (RAG2-KO) or TCR δ -KO host. (f) Comparative surface expression of the indicated markers in CD122⁻NK1.1⁻ versus CD122⁺NK1.1⁺ cells gated on WT TCR $\gamma\delta$ ⁺CD3⁺CD27⁺ splenocytes. (g,h) Intracellular IFN- γ expression (after PMA and ionomycin stimulation) in TCR $\gamma\delta$ ⁺CD3⁺CD27⁺ splenocytes (g) and parasitemia as percentage of blood GFP⁺ cells (h, $n = 5$ mice) 5 d after infection with *P. berghei* ANKA sporozoites. Numbers above plots (g) indicate mean \pm s.d. absolute counts of IFN- γ ⁺ $\gamma\delta$ cells. (i) Survival curves of mice infected as in (g) ($n = 10$ mice in two independent experiments). NS, not significant; * $P < 0.05$, ** $P < 0.01$ (Student's *t*-test). Data in a–i are representative of three independent experiments. Error bars indicate mean \pm s.d.; dots represent individual mice. Numbers in outlined areas or quadrants of flow cytometry plots indicate percentages of cells in each.

subsets³². V γ 6⁺ thymocytes have been shown to outcompete V γ 4⁺ thymocytes when reconstituting the dermis of $\gamma\delta$ T-cell-deficient mice⁸, and whereas fetal-derived (and thymically programmed) V γ 6⁺ T cells were shown to be resident in the dermis, adult BM-derived V γ 4⁺ T cells seem to depend on extrathymic signals to migrate to the skin. Thus, by differentially controlling tissue homing properties, thymic programming may determine the pathophysiological contributions of discrete $\gamma\delta$ T cell subsets. Consistent with this, V γ 4⁺ T cells represent the major source of IL-17 in psoriasis-like inflammation^{8,32}, as well as in experimental autoimmune encephalomyelitis¹³ and collagen-induced arthritis⁴⁶, whereas V γ 6⁺ T cells are more frequent in *Listeria* infection⁵ and ovarian cancer¹⁸.

The observation that fetal-derived and adult IL-17⁺ $\gamma\delta$ T cells have distinct TCR signaling requirements could not be made with the available (V γ 4-based) transgenic TCR $\gamma\delta$ models and resolves previous controversies on the TCR dependence (or independence) of IL-17⁺ $\gamma\delta$ T cell development^{12,21,22,28}. Namely, our data indicate that V γ 6⁺, but not V γ 4⁺, thymocytes depend on strong TCR signals for functional differentiation, which in turn warrants investigation into their respective ligand engagement requirements.

In addition to ligand engagement, distinct signaling cascades downstream of the TCR $\gamma\delta$ may differentially affect $\gamma\delta$ T cell subsets. It will be important to establish whether TCR $\gamma\delta$ signaling is perceived mostly quantitatively or qualitatively on the basis of the engagement of distinct signaling pathways, such as ERK-MAPK or PI3K-AKT (N. Sumaria, B.S.-S. and D.J.P., unpublished data). Further downstream in cellular programming, our transcriptional analysis of fetal and adult total $\gamma\delta$ thymocytes stages showed that CD3DH $\gamma\delta$ thymocytes efficiently downregulated the IL-17 program but were deficient in upregulating the IFN- γ pathway between fetal and adult stages. Particularly affected were the transcription factors *Egr2*, *Egr3* and *Id3*, which are induced by agonist TCR signaling^{21,47} and may be required to suppress a 'default' ROR γ t-dependent IL-17 program and maximize IFN- γ production in $\gamma\delta$ thymocytes. This would be consistent with both the repression of the IL-17 pathway in V γ 5⁺ DETC development²¹ and the depletion, in CD3DH mice, of V γ 1-biased CD27⁺CD122⁺NK1.1⁺ $\gamma\delta$ T cells, the subset expressing the highest IFN- γ on a per cell basis.

Notably, the transcription factors that control *Ifng* and *Il17a* expression, T-bet and ROR γ t, were normally expressed in CD3DH $\gamma\delta$

T cell subsets, suggesting that the $\gamma\delta$ T cell differentiation phenotype in these mice derives from mechanisms downstream of T-bet or ROR γ t expression. This is in agreement with normal expression of these transcription factors in $\gamma\delta$ thymocytes deficient for the TCR signal transducer Itk²⁸. We therefore propose that a major function of TCR $\gamma\delta$ signaling is to select preprogrammed precursors, which could resemble innate lymphoid cells (ILCs), for differentiation into effector cells making IFN- γ or IL-17. Future studies on the functional similarities and differences between ILC and $\gamma\delta$ T cell subsets may contribute to understanding the evolutionary conservation of these innate-like lymphocytes and their therapeutic potential for infectious or inflammatory diseases and cancer²⁰.

METHODS

Methods and any associated references are available in the [online version of the paper](#).

Accession codes. Gene Expression Omnibus: Microarray data have been deposited under accession code [GSE71637](#).

Note: Any Supplementary Information and Source Data files are available in the online version of the paper.

ACKNOWLEDGMENTS

We thank K. Serre, J. Martins, N. Schmolka, A. Amorim, V.Z. Luís and M.M. Mota (all at iMM Lisboa); and B. Garcillán, D. de Juan, M. Mazariegos, M. Sanz-Rodríguez and S. Díaz-Castroverde (Complutense University) for help and advice; A. Hayday (King's College London) and P. Pereira (Pasteur Institute) for insightful discussions; and the staff of the animal and flow cytometry facilities at iMM Lisboa and Complutense University for technical assistance. This work was funded by the European Research Council (StG_260352 and CoG_646701 to B.S.-S.); MINECO (SAF2011-24235 and BES-2012-055054 to J.R.R.), CAM (S2010/BMD-2316/2326 to J.R.R.) and the Lair Foundation (2012/0070 to J.R.R.); and FIS PI11/02198 and MINECO SAF2014-54708-R to E.F.-M.

AUTHOR CONTRIBUTIONS

M.M.-R., B.S.-S., E.F.-M., J.R.R. and D.J.P. designed research; M.M.-R., J.C.R., A.R.G., N.G.-S. and A.P. performed experiments; B.S.-S., E.F.-M. and J.R.R. supervised research and wrote the manuscript.

COMPETING FINANCIAL INTERESTS

The authors declare no competing financial interests.

Reprints and permissions information is available online at <http://www.nature.com/reprints/index.html>.

- Wang, T. *et al.* IFN- γ -producing $\gamma\delta$ T cells help control murine West Nile virus infection. *J. Immunol.* **171**, 2524–2531 (2003).
- Gao, Y. *et al.* $\gamma\delta$ T cells provide an early source of interferon- γ in tumor immunity. *J. Exp. Med.* **198**, 433–442 (2003).
- Jagannathan, P. *et al.* Loss and dysfunction of V δ 2⁺ $\gamma\delta$ T cells are associated with clinical tolerance to malaria. *Sci. Transl. Med.* **6**, 251ra117 (2014).
- Cho, J.S. *et al.* IL-17 is essential for host defense against cutaneous *Staphylococcus aureus* infection in mice. *J. Clin. Invest.* **120**, 1762–1773 (2010).
- Sheridan, B.S. *et al.* $\gamma\delta$ T cells exhibit multifunctional and protective memory in intestinal tissues. *Immunity* **39**, 184–195 (2013).
- Cai, Y. *et al.* Pivotal role of dermal IL-17-producing $\gamma\delta$ T cells in skin inflammation. *Immunity* **35**, 596–610 (2011).
- Pantelyushin, S. *et al.* Ror γ t⁺ innate lymphocytes and $\gamma\delta$ T cells initiate psoriasisiform plaque formation in mice. *J. Clin. Invest.* **122**, 2252–2256 (2012).
- Cai, Y. *et al.* Differential developmental requirement and peripheral regulation for dermal V γ 4 and V γ 6T17 cells in health and inflammation. *Nat. Commun.* **5**, 3986 (2014).
- Park, S.G. *et al.* T regulatory cells maintain intestinal homeostasis by suppressing $\gamma\delta$ T cells. *Immunity* **33**, 791–803 (2010).
- Romani, L. *et al.* Defective tryptophan catabolism underlies inflammation in mouse chronic granulomatous disease. *Nature* **451**, 211–215 (2008).
- Shichita, T. *et al.* Pivotal role of cerebral interleukin-17-producing $\gamma\delta$ T cells in the delayed phase of ischemic brain injury. *Nat. Med.* **15**, 946–950 (2009).
- Jensen, K.D. *et al.* Thymic selection determines $\gamma\delta$ T cell effector fate: antigen-naïve cells make interleukin-17 and antigen-experienced cells make interferon- γ . *Immunity* **29**, 90–100 (2008).
- Sutton, C.E. *et al.* Interleukin-1 and IL-23 induce innate IL-17 production from $\gamma\delta$ T cells, amplifying Th17 responses and autoimmunity. *Immunity* **31**, 331–341 (2009).
- Petermann, F. *et al.* $\gamma\delta$ T cells enhance autoimmunity by restraining regulatory T cell responses via an interleukin-23-dependent mechanism. *Immunity* **33**, 351–363 (2010).
- Prinz, I., Silva-Santos, B. & Pennington, D.J. Functional development of $\gamma\delta$ T cells. *Eur. J. Immunol.* **43**, 1988–1994 (2013).
- Ribot, J.C. *et al.* CD27 is a thymic determinant of the balance between interferon- γ and interleukin 17-producing $\gamma\delta$ T cell subsets. *Nat. Immunol.* **10**, 427–436 (2009).
- Haas, J.D. *et al.* CCR6 and NK1.1 distinguish between IL-17A and IFN- γ -producing $\gamma\delta$ effector T cells. *Eur. J. Immunol.* **39**, 3488–3497 (2009).
- Rei, M. *et al.* Murine CD27⁻ V γ 6⁺ $\gamma\delta$ T cells producing IL-17A promote ovarian cancer growth via mobilization of protumor small peritoneal macrophages. *Proc. Natl. Acad. Sci. USA* **111**, E3562–E3570 (2014).
- Wu, P. *et al.* $\gamma\delta$ T17 cells promote the accumulation and expansion of myeloid-derived suppressor cells in human colorectal cancer. *Immunity* **40**, 785–800 (2014).
- Silva-Santos, B., Serre, K. & Norell, H. $\gamma\delta$ T cells in cancer. *Nat. Rev. Immunol.* **15**, 683–691 (2015).
- Turchinovich, G. & Hayday, A.C. Skint-1 identifies a common molecular mechanism for the development of interferon- γ -secreting versus interleukin-17-secreting $\gamma\delta$ T cells. *Immunity* **35**, 59–68 (2011).
- Wencker, M. *et al.* Innate-like T cells straddle innate and adaptive immunity by altering antigen-receptor responsiveness. *Nat. Immunol.* **15**, 80–87 (2014).
- Ciofani, M. & Zúñiga-Pflücker, J.C. Determining $\gamma\delta$ versus $\alpha\beta$ T cell development. *Nat. Rev. Immunol.* **10**, 657–663 (2010).
- Haks, M.C. *et al.* Attenuation of $\gamma\delta$ TCR signaling efficiently diverts thymocytes to the $\alpha\beta$ lineage. *Immunity* **22**, 595–606 (2005).
- Hayes, S.M., Li, L. & Love, P.E. TCR signal strength influences $\alpha\beta/\gamma\delta$ lineage fate. *Immunity* **22**, 583–593 (2005).
- O'Brien, R.L. & Born, W.K. $\gamma\delta$ T cell subsets: a link between TCR and function? *Semin. Immunol.* **22**, 193–198 (2010).
- Narayan, K. *et al.* & Immunological Genome Project Consortium. Intrathymic programming of effector fates in three molecularly distinct $\gamma\delta$ T cell subtypes. *Nat. Immunol.* **13**, 511–518 (2012).
- Malhotra, N. *et al.* & Immunological Genome Project Consortium. A network of high-mobility group box transcription factors programs innate interleukin-17 production. *Immunity* **38**, 681–693 (2013).
- Dave, V.P. *et al.* CD3 δ deficiency arrests development of the $\alpha\beta$ but not the $\gamma\delta$ T cell lineage. *EMBO J.* **16**, 1360–1370 (1997).
- Coffey, F. *et al.* The TCR ligand-inducible expression of CD73 marks $\gamma\delta$ lineage commitment and a metastable intermediate in effector specification. *J. Exp. Med.* **211**, 329–343 (2014).
- Azzam, H.S. *et al.* CD5 expression is developmentally regulated by T cell receptor (TCR) signals and TCR avidity. *J. Exp. Med.* **188**, 2301–2311 (1998).
- Haas, J.D. *et al.* Development of interleukin-17-producing $\gamma\delta$ T cells is restricted to a functional embryonic wave. *Immunity* **37**, 48–59 (2012).
- Schmolka, N. *et al.* Epigenetic and transcriptional signatures of stable versus plastic differentiation of proinflammatory $\gamma\delta$ T cell subsets. *Nat. Immunol.* **14**, 1093–1100 (2013).
- Schmolka, N., Wencker, M., Hayday, A.C. & Silva-Santos, B. Epigenetic and transcriptional regulation of $\gamma\delta$ T cell differentiation: programming cells for responses in time and space. *Semin. Immunol.* **27**, 19–25 (2015).
- Silva-Santos, B., Pennington, D.J. & Hayday, A.C. Lymphotoxin-mediated regulation of $\gamma\delta$ cell differentiation by $\alpha\beta$ T cell progenitors. *Science* **307**, 925–928 (2005).
- Kannan, Y. *et al.* I κ B ζ augments IL-12- and IL-18-mediated IFN- γ production in human NK cells. *Blood* **117**, 2855–2863 (2011).
- Gu, X. *et al.* The gp49B1 inhibitory receptor regulates the IFN-gamma responses of T cells and NK cells. *J. Immunol.* **170**, 4095–4101 (2003).
- Ribot, J.C. *et al.* Cutting edge: adaptive versus innate receptor signals selectively control the pool sizes of murine IFN- γ or IL-17-producing $\gamma\delta$ T cells upon infection. *J. Immunol.* **185**, 6421–6425 (2010).
- D'Ombra, M.C., Hansen, D.S., Simpson, K.M. & Schofield, L. $\gamma\delta$ -T cells expressing NK receptors predominate over NK cells and conventional T cells in the innate IFN- γ response to *Plasmodium falciparum* malaria. *Eur. J. Immunol.* **37**, 1864–1873 (2007).
- Hayes, S.M. & Love, P.E. Stoichiometry of the murine $\gamma\delta$ T cell receptor. *J. Exp. Med.* **203**, 47–52 (2006).
- Siegers, G.M. *et al.* Different composition of the human and the mouse $\gamma\delta$ T cell receptor explains different phenotypes of CD3 γ and CD3 δ immunodeficiencies. *J. Exp. Med.* **204**, 2537–2544 (2007).
- Zapata, D.A. *et al.* Conformational and biochemical differences in the TCR-CD3 complex of CD8⁺ versus CD4⁺ mature lymphocytes revealed in the absence of CD3 γ . *J. Biol. Chem.* **274**, 35119–35128 (1999).
- Fernández-Malavé, E. *et al.* Overlapping functions of human CD3 δ and mouse CD3 γ in $\alpha\beta$ T-cell development revealed in a humanized CD3 γ -mouse. *Blood* **108**, 3420–3427 (2006).
- Hayes, S.M. *et al.* Activation-induced modification in the CD3 complex of the $\gamma\delta$ T cell receptor. *J. Exp. Med.* **196**, 1355–1361 (2002).
- Hayes, S.M. & Love, P.E. Distinct structure and signaling potential of the $\gamma\delta$ TCR complex. *Immunity* **16**, 827–838 (2002).
- Roark, C.L. *et al.* Exacerbation of collagen-induced arthritis by oligoclonal, IL-17-producing $\gamma\delta$ T cells. *J. Immunol.* **179**, 5576–5583 (2007).
- Seiler, M.P. *et al.* Elevated and sustained expression of the transcription factors Egr1 and Egr2 controls NKT lineage differentiation in response to TCR signaling. *Nat. Immunol.* **13**, 264–271 (2012).

ONLINE METHODS

Mice. Adult mice were used at 4–8 weeks of age. Embryos were obtained by the setting up of timed pregnancies. C57BL/6 (wild-type (WT)) mice were from Charles River Laboratories. *Cd3g*^{-/-} mice have been described⁴⁸ and were a gift from D. Kappes (Fox Chase Cancer Center). *Cd3δ*^{-/-} have been described²⁹ and were a gift from I. Luescher (Ludwig Institute for Cancer Research). CD3DH mice were obtained by crossing *Cd3g*^{-/-} males with *Cd3δ*^{-/-} females. For the studies, both males and females were used. Mice were bred and maintained in the pathogen-free animal facilities of the Instituto de Medicina Molecular (Lisbon) and Animalario Universidad Complutense (Madrid). All experiments involving animals were done in compliance with the relevant laws and institutional guidelines. Experimental procedures were approved by the Ethics Committee for Animal Experimentation of Universidad Complutense and Comunidad de Madrid, and by the institutional animal welfare body (ORBEA-IMM) and by the DGAV (Portuguese competent authority for animal protection), all in accordance with Directive 2010/63/EU.

Bone marrow chimeras. *Rag2*^{-/-} or *Tcrd*^{-/-} mice were lethally irradiated (900 rad), and the next day injected intravenously with a total of 10⁷ whole bone marrow cells of mixed (1:1 or 1:9) WT (Thy-1.1) and CD3DH (Thy-1.2) origin. Chimeras were given antibiotic-containing water (2% Bactrim; Roche) for the first 4 weeks after irradiation. The hematopoietic compartment was allowed to reconstitute for 6 weeks before organs were harvested for flow cytometry analysis.

Cell preparations. Thymi, lymph nodes and spleens were homogenized and washed in RPMI medium containing 10% (vol/vol) FCS. Splenocytes were depleted from erythrocytes using the Red Blood Cell Lysis buffer 1× (BioLegend).

Monoclonal antibodies. All antibodies used are described in **Supplementary Table 1**.

Flow cytometry and cell sorting. For cell surface staining, thymocytes, erythrocyte-depleted splenocytes or lymph node cells were incubated for 30 min with saturating concentrations of monoclonal antibodies (mAbs) (**Supplementary Table 1**). For intracellular cytokine staining, cells were stimulated with PMA (50 ng/mL) and ionomycin (1 μg/mL), in the presence of Brefeldin A (10 μg/mL) (all from Sigma) for 4 h at 37 °C. Cells were stained for the identified above cell surface markers, fixed 30 min at 4 °C and permeabilized with the Foxp3/Transcription Factor Staining Buffer set (eBioscience) in the presence of anti-CD16/CD32 (93) (eBioscience) for 15 min at 4 °C, and finally incubated for 1 h at room temperature with identified above cytokine-specific antibodies in permeabilization buffer. Samples were acquired using FACSFortessa (BD Biosciences). Data were analyzed using FlowJo software (Tree Star). Live indicated subsets were electronically sorted when indicated using FACSAria (BD Biosciences).

Cell culture. For early activation markers, cells were incubated for 24 h on plate-bound anti-CD3e (10 mg/ml) and analyzed by flow cytometry. For phosphorylated molecules downstream of TCR and isotype-matched

control antibody, sorted lymph node cells were stimulated for 5 min with soluble anti-CD3e (10 μg/ml) then fixed for 30 min at 4 °C and permeabilized with the Foxp3/Transcription Factor Staining Buffer set (eBioscience) in the presence of anti-CD16/CD32 Fc Block (93) (eBioscience) for 30 min at room temperature and finally incubated for 1 h at room temperature with anti-p-ERK in permeabilization buffer. For T_H1 cell polarization, CD4⁺ αβ T cells were isolated by flow cytometry and incubated for 4 d on plate-bound anti-CD3e and anti-CD28 (5 ng/ml each). When indicated (T_H1 cocktail), the following cytokines and neutralizing antibodies were added to the culture milieu: IL-2 (10 ng/ml; Preprotech), IL-12 (50 ng/ml; Preprotech) and anti-IL-4 (11B11) (10 μg/ml; eBioscience).

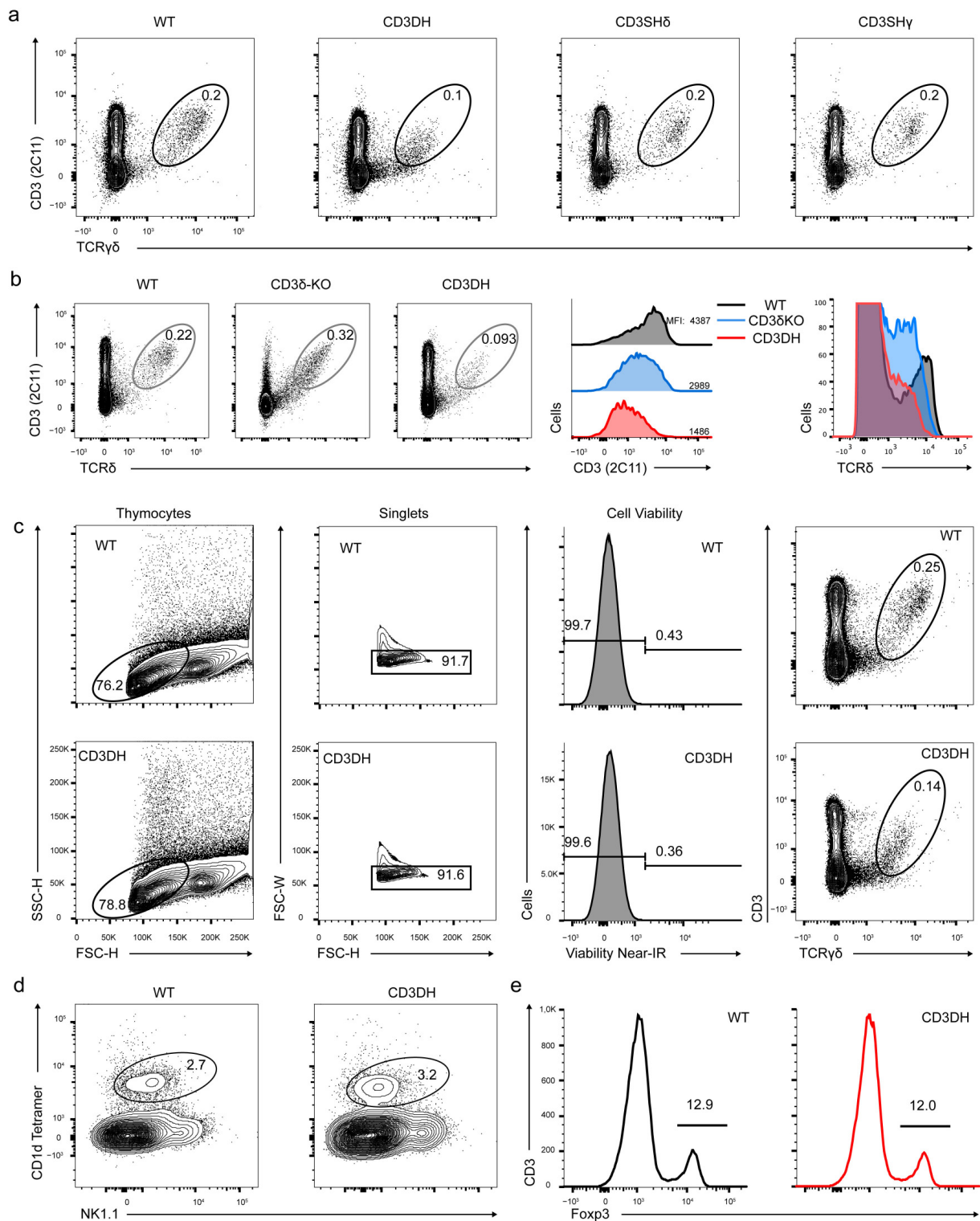
Malaria infection. Mice were infected as described⁴⁹.

RNA isolation, cDNA production and real-time PCR. Total RNA was extracted using the RNeasy Mini kit (Qiagen) according to the manufacturer's instructions. Concentration and purity were determined using the NanoDrop ND-1000 spectrophotometer (Thermo Scientific). Total RNA was reverse transcribed into cDNA using a Transcriptor High Fidelity cDNA Synthesis kit (Roche). Quantitative real-time PCR was performed on ViiA 7 Real-Time PCR system (Applied Biosystems; Life Technologies). Primers were either designed manually or by the Universal ProbeLibrary Assay Design Center (Roche). Sequences are available upon request. Analysis of quantitative PCR results was performed using the ViiA 7 software v1.2 (Applied Biosystems; Life Technologies).

Microarray. All microarray data analysis was done with R and several packages available from CRAN⁵⁰ and Bioconductor⁵¹. The raw data (CEL files) were normalized and summarized with the Robust MultiArray Average method implemented in the 'oligo' package⁵². Variations in gene expression levels were determined using 'limma' package⁵³ and only genes with fold-change >2 were considered for downstream analysis.

Statistical analysis. The statistical significance of differences between populations was assessed with the Student's *t*-test; *P* < 0.05 was considered significant. Mouse sample sizes were chosen to ensure significance of *t*-test. No mice were excluded. No randomization or blinding was performed. Data met normal distribution with similar variance between groups.

48. Haks, M.C., Krimpenfort, P., Borst, J. & Kruisbeek, A.M. The CD3γ chain is essential for development of both the TCRαβ and TCRγδ lineages. *EMBO J.* **17**, 1871–1882 (1998).
49. Liehl, P. *et al.* Host-cell sensors for *Plasmodium* activate innate immunity against liver-stage infection. *Nat. Med.* **20**, 47–53 (2014).
50. R Development Core Team. R: a language and environment for statistical computing (R Foundation for Statistical Computing, Vienna, Austria, 2011).
51. Huber, W. *et al.* Orchestrating high-throughput genomic analysis with Bioconductor. *Nat. Methods* **12**, 115–121 (2015).
52. Carvalho, B.S. & Irizarry, R.A. A framework for oligonucleotide microarray preprocessing. *Bioinformatics* **26**, 2363–2367 (2010).
53. Ritchie, M.E. *et al.* limma powers differential expression analyses for RNA-sequencing and microarray studies. *Nucleic Acids Res.* **43**, e47 (2015).

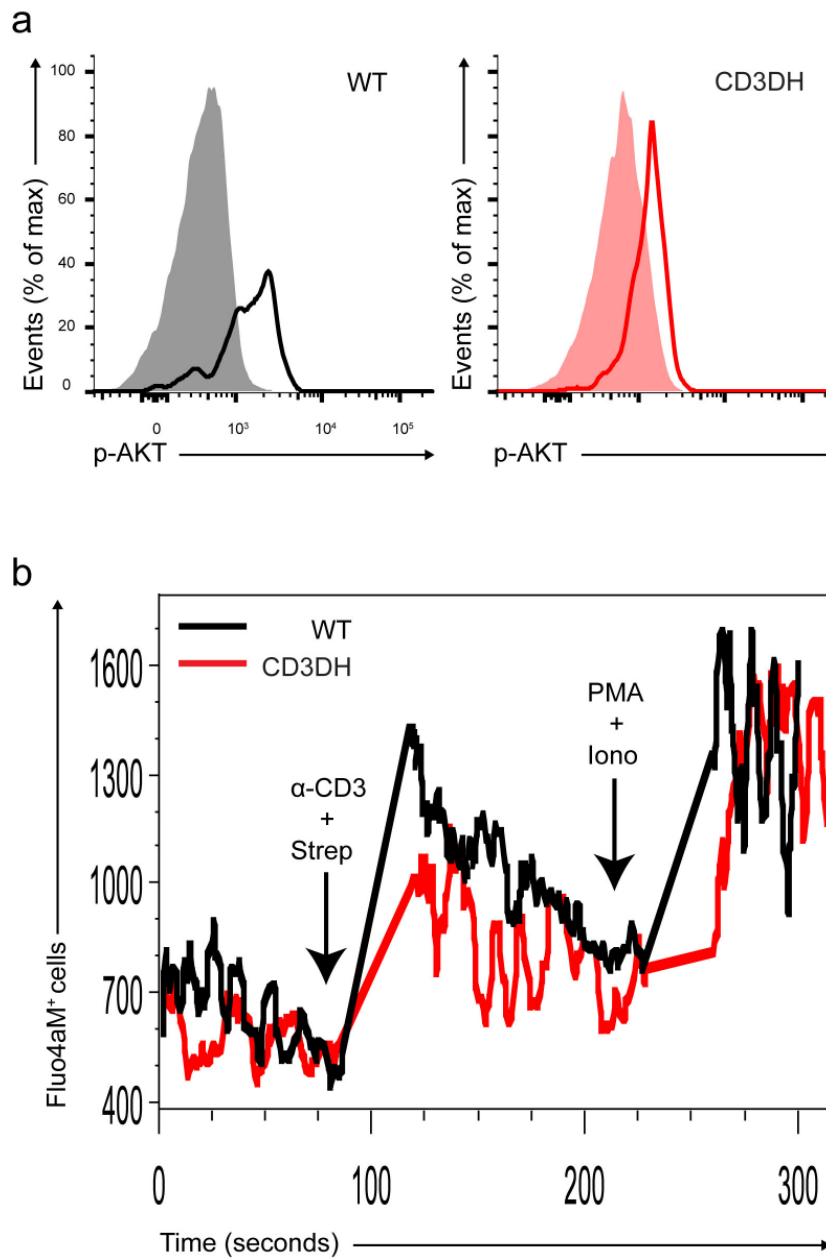


Supplementary Figure 1

$\gamma\delta$ and $\alpha\beta$ T cell development in CD3 mutant mice.

(a) Flow cytometry showing the CD3 ϵ vs TCR δ phenotype of thymocytes from adult WT or CD3SH (single heterozygote for CD3 δ or

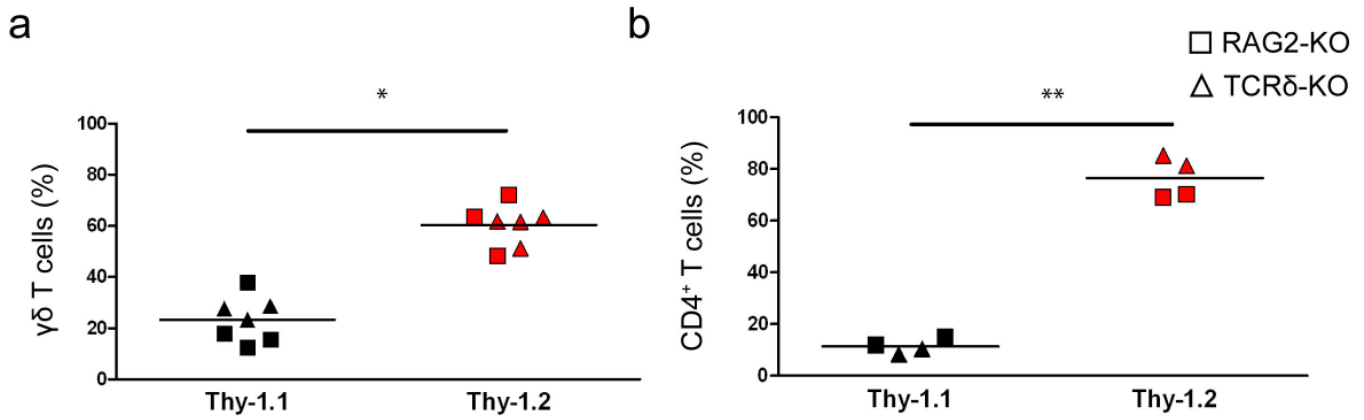
CD3 γ) mice (n = 3 per group). Numbers within gated areas indicate % cells in each throughout. **(b)** Left, representative CD3 ϵ vs TCR δ phenotype of thymocytes from the indicated adult mice. Numbers as in (a). Right, CD3 ϵ and TCR δ expression (MFI) in gated TCR δ ⁺ thymocytes and CD3⁺ thymocytes, respectively, from the indicated adult mice (n = 3 per group). Numbers indicate MFI **(c)** Gating strategy for CD3⁺ TCR δ ⁺ $\gamma\delta$ T cell identification. Doublets and dead cells were excluded. **(d, e)** Comparative analysis of TCR β ⁺CD1d⁺ NKT cells (d) and CD4⁺Foxp3⁺ Treg cells (e) in WT and CD3DH mice. Numbers in c, d, and e indicate percentage of cells within the marked region.



Supplementary Figure 2

$\gamma\delta$ T cells from CD3DH mice show impaired TCR $\gamma\delta$ signaling.

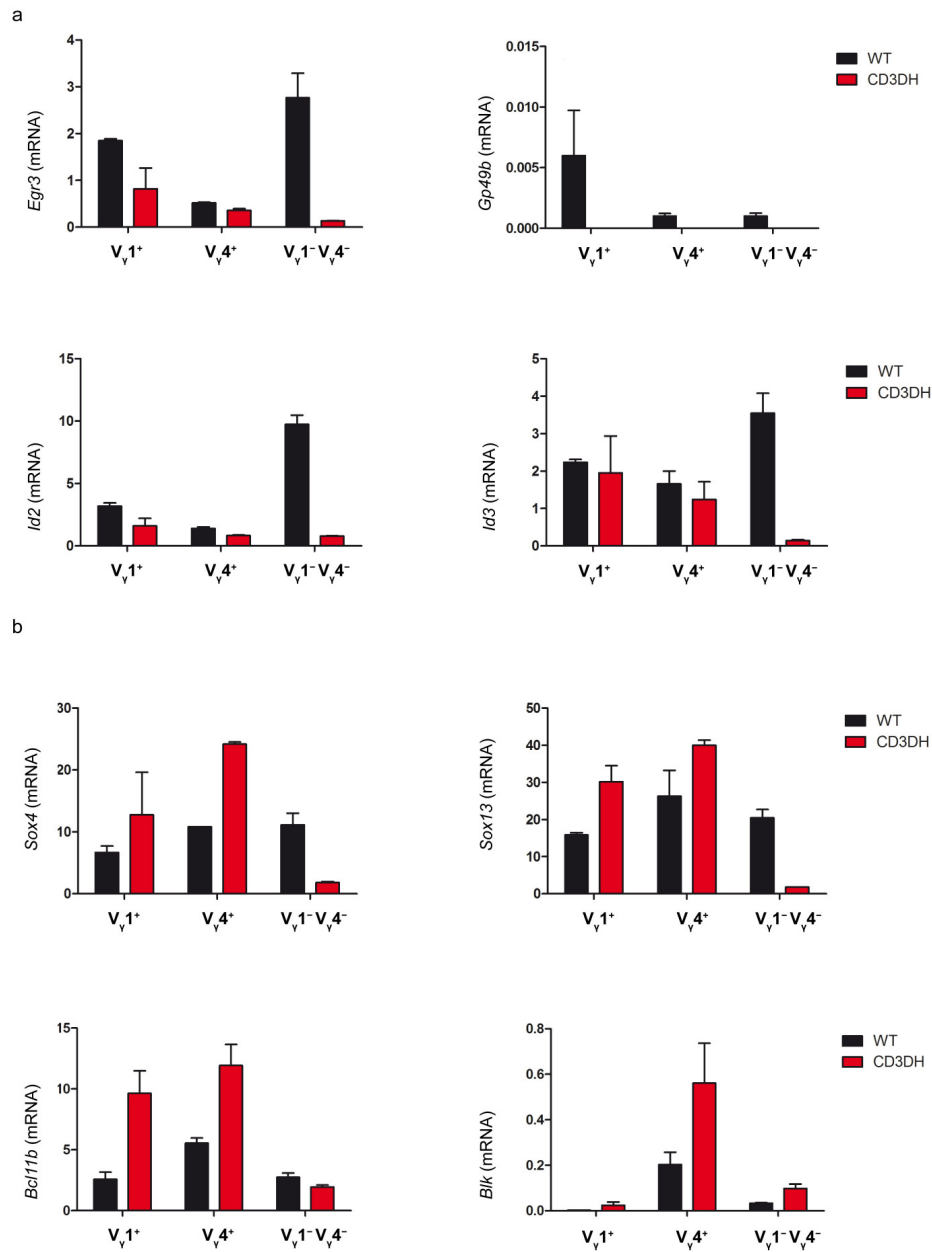
(a) Flow cytometry of phosphorylated AKT (empty histograms) in sorted TCR δ^+ CD3 $^+$ CD27 $^+$ lymph node cells from the indicated mice, after 5 min stimulation with PMA plus ionomycin; filled histograms represent staining with isotype-matched control antibody. (b) Intracellular calcium mobilization in TCR δ^+ CD3 $^+$ CD27 $^+$ lymph node cells obtained from the indicated mice, after 5 min stimulation with 10 μ g/ml biotinylated anti-CD3 ϵ mAb followed by TCR crosslinking with 10 μ g/ml streptavidin, and then assessed over 5 min, followed by 2 min stimulation with PMA plus ionomycin.



Supplementary Figure 3

Contributions of WT or CD3DH progenitors to $\gamma\delta$ and $CD4^+$ thymocytes in mixed bone marrow chimeras.

Thy-1.1⁺ (WT-derived) vs Thy-1.2⁺ (CD3DH-derived) fractions within TCR δ^+ CD3⁺ thymocytes (**a**) and CD4⁺CD3⁺ thymocytes (**b**) from 1:9 mixed WT:CD3DH BM chimeras. Each symbol indicates one individual host, either RAG2^{-/-} (squares) or TCR δ ^{-/-} (triangles). *P < 0.01, **P < 0.001 (Student's t-test). Data are from three independent experiments.

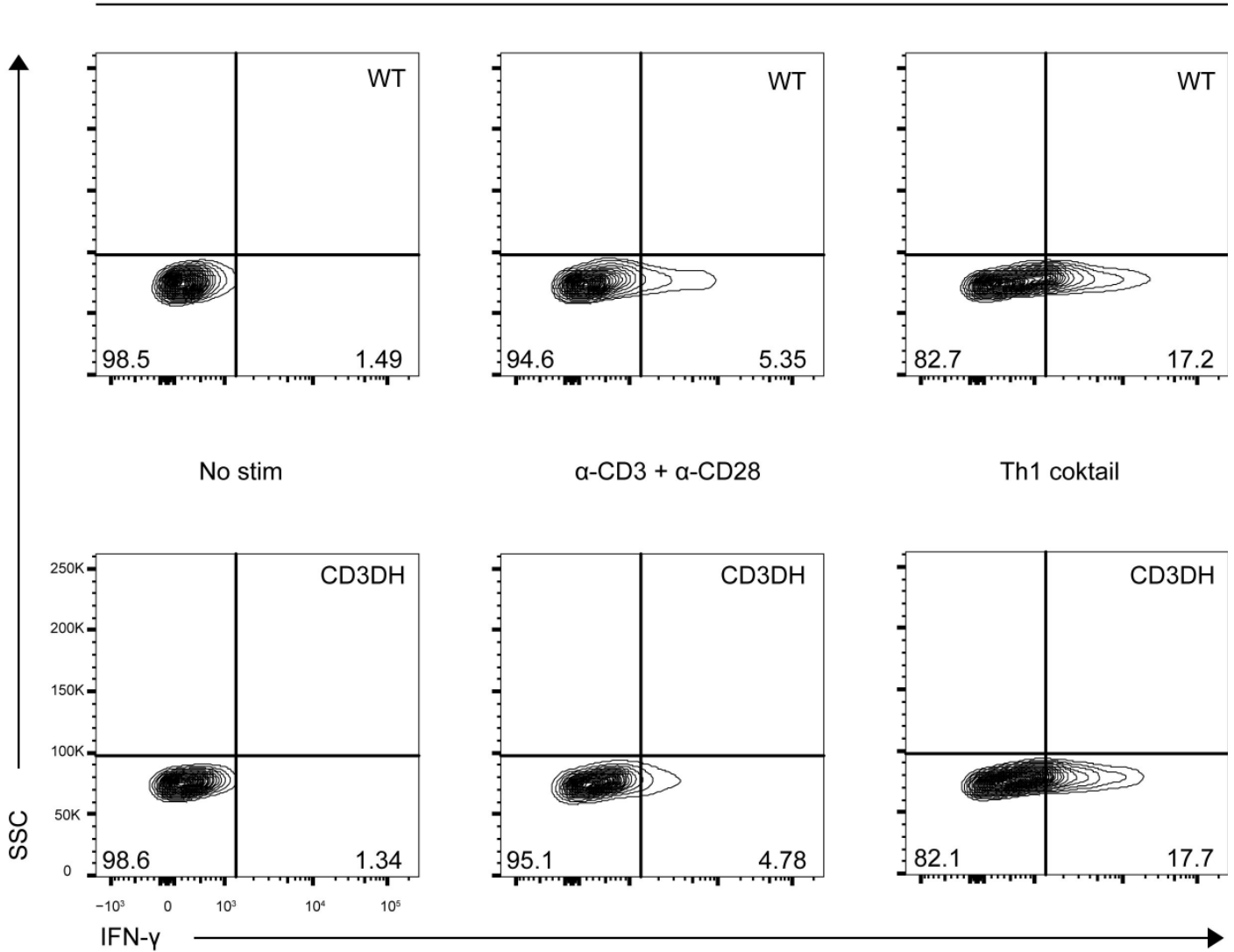


Supplementary Figure 4

Transcriptional signatures of V_γ-based γδ thymocyte subsets.

Relative expression of *Egr3*, *Id2*, *Id3* and *Gp49b* (a) or *Sox4*, *Sox13*, *Bcl11b* and *Blk* (b), in arbitrary units normalized to the housekeeping gene *hprt*, in sorted V_γ1⁺, V_γ4⁺ or V_γ1⁻V_γ4⁻ thymocytes from either WT or CD3DH E18 embryos. Data shown are the mean +/- s.d.

CD4⁺ TCRαβ⁺ cells



Supplementary Figure 5

CD4⁺ T cells from CD3DH mice differentiate normally into T_H1 cells.

(a) Flow cytometry of intracellular IFN-γ expression of WT (top) and CD3DH (bottom) TCRβ⁺CD4⁺ splenocytes incubated for 4 days without stimuli (left panels) or on plate-bound α-CD3ε and α-CD28 mAb (5ng/ml each), without (middle panels) or with (right panels) Th1-polarizing cytokines IL-2 (10 ng/ml) and IL-12 (50 ng/ml) plus anti-IL-4 (10 μg/mL) neutralizing antibody. Numbers indicate % of cells in each quadrant. Data are representative of two independent experiments.

Specificity	Clon	Fluorochrome	1DB_ID:	Origin
CD3	145.2C11	PerCPCy5.5	1DB-001-0000264176	eBioscience
CD3	17A2	APC-Cy7	1DB-001-0000263478	eBioscience
CD3	145.2C11	Pure	1DB-001-0000264178	eBioscience
CD3	17A2	Pure	1DB-001-0000226069	eBioscience
CD4	GK1.5	FITC	1DB-001-0000263406	eBioscience
CD4	RM4-5	PerCPCy5.5	1DB-001-0000884856	eBioscience
CD5	53-7.3	PE	1DB-001-0000263310	eBioscience
CD8	53.6.7	APC-Cy7	1DB-001-0000263248	eBioscience
CD24	M1/69	PB	1DB-001-0000263563	eBioscience
CD25	PC61	Pe-Cy7	1DB-001-0001017649	eBioscience
CD25	PC61	APC	1DB-001-0001111370	eBioscience
CD25	PC61	APC-Cy7	1DB-001-0001111736	eBioscience
CD27	LG.7F9	PE	1DB-001-0000840049	Biologend
CD27	LG.7F9	Pe-Cy7	1DB-001-0001111490	eBioscience
CD27	LG.3A10	PerCPCy5.5	1DB-001-0000840053	Biologend
CD27	LG.7F9	APC	1DB-001-0000840051	Biologend
CD44	IM7	PE	1DB-001-0000262159	eBioscience
CD44	IM7	PerCPCy5.5	1DB-001-0000838541	Biologend
CD45RB	16A	PE	1DB-001-0000869761	BDPharmigen
CD62L	MEL-14	APC	1DB-001-0000263293	eBioscience
CD69	H1.2F3	APC	1DB-001-0000264162	eBioscience
CD73	AD2	PE	1DB-001-0000873094	BDPharmigen
CD122	TM-β1	FITC	1DB-001-0000263783	eBioscience
CD122	TM-β1	FITC	1DB-0010000839954	Biologend
TCRδ	GL3	PE	1DB-001-0000264125	eBioscience
TCRδ	GL3	PerCPCy5.5	1DB-001-0000862611	Biologend
TCRδ	GL3	BV 421	1DB-001-0000862613	eBioscience
Vγ1	2.11	APC	1DB-001-0001061965	Biologend
Vγ4	UC3-10A6	FITC	1DB-001-0000884592	BDPharmigen
IFNγ	XMG1.2	PE	1DB-001-0001110823	eBioscience
IL17A	TC11.18H10.1	PB	1DB-001-0000845132	Biologend
NK1.1	PK136	Pe-Cy7	1DB-001-0000263921	eBioscience
ERK	XMG1.2	PE	1DB-001-0000869045	BDPharmigen

Supplemental Table 1. List of antibodies